International Journal of Mass Spectrometry 312 (2012) 87–96

Contents lists available at ScienceDirect

International Journal of Mass Spectrometry

journal homepage: www.elsevier.com/locate/ijms

# Characterization of cofactors, substrates and inhibitor binding to flavoenzyme quinone reductase 2 by automated supramolecular nano-electrospray ionization mass spectrometry

Mathias Antoine[a], Estelle Marcheteau[a], Philippe Delagrange[b], Gilles Ferry[a], Jean A. Boutin[a,*]

[a] Biotechnologie, Pharmacologie Moléculaire et Cellulaire, France
[b] Département des Sciences Expérimentales, Institut de Recherches Servier, 125 Chemin de Ronde, 78290 Croissy-sur-Seine, France

ARTICLE INFO

*Article history:*
Received 14 March 2011
Received in revised form 1 July 2011
Accepted 11 July 2011
Available online 21 July 2011

*Keywords:*
Supramolecular mass spectrometry
Quinone reductase
Flavoprotein
Resveratrol
Melatonin

ABSTRACT

Quinone reductase 2 (QR2) is a cytosolic homodimeric enzyme implicated in the reduction of quinone in the presence of natural derivatives of NADH such as *N*-ribosyldihydronicotinamide. QR2 does not recognize NADH or NADPH as co-substrates, unlike quinone reductase 1 (QR1). This feature is not the only unusual one of this enzyme. Although it resembles quinone reductase 1, the well-described detoxifying enzyme, QR2 does not share many features with QR1. Particularly, it does not seem to have a similar detoxifying function in cells. Therefore, starting from basic knowledge on QR2 and adding up to previous works published on the enzyme, we wanted to rebuild its biochemical description because some of the recently described characteristics are surprising, and merit further explorations. For example, QR2 seems to be over-expressed in neurodegenerative diseases, and this over-expression seems to be linked to a worsening of the pathological conditions. Indeed, our specific inhibitors of QR2, tested *in vivo*, show outstanding properties impairing memory loss. These observations led us to further describe, at the molecular level, the relationship between QR2 and some of its inhibitors and co-substrates. In the present paper, we address this question using non-denaturing supramolecular nano-electrospray ionization mass spectrometry. This characterization helps understand the physical relationship between inhibitors such as resveratrol or melatonin and the enzyme.



## 1. Introduction

Quinone reductase 2 (QR2, E.C. 1.10.99.2) is a cytosolic enzyme with many enigmatic features [1]. Its main recognized activity would be the catalysis of a detoxification process for quinones. For at least two reasons, this activity is not validated. Firstly, QR2 is a close neighbour of QR1 (DT-diaphorase) that is, beyond any doubt, a detoxification enzyme. QR1 and QR2 are closely related [2], since they share 59% (cDNA) and 44% (protein) similarity in their sequences, with the interesting difference that QR1 has a 43 amino acid longer C-terminus than QR2 [3]. Due to this particular fact, QR2 does not recognize NADH and NADPH as co-substrates but rather natural compounds possibly derived from those, such as *N*-ribosyl- or *N*-methyl-dihydronicotinamide [4,5]. Secondly, two papers are absolutely crucial in understanding the role of QR1 and QR2 in animals. Those papers described the toxicity of menadione in wild type *versus* genetic knock out animals. For each of those enzyme genetic deletions, the net results are that menadione is toxic in wt animals, but less toxic in mice genetically deleted of the QR2 gene and more toxic in mice genetically deleted of the QR1 gene [6,7]. This observation (that was independently obtained in our own laboratory on our own, independently obtained, genetically deleted QR2 mice ([8], [Delagrange & Boutin, unpublished]) could be reasonably attributed to a harmful action of QR2 in the presence of menadione. Therefore, an unsolved question, so far, is the role of QR2 in physiology. In standard – and equivalent – situations, it seems that QR2 leads to the production of far more radical oxygen species (ROS) than QR1 [9]. The only difference between those two situations – aside from the sequence itself, obviously – is that, as stated before, QR1 uses standard hydride donors (NADH/NAD(P)H), while QR2 uses exotic ones, from either natural (*N*-ribosylnicotinamide or *N*-methylnicotinamide) or synthetic (*N*-benzylnicotinamide) origins. As of today, the abundance and role of the natural and putative co-substrates of QR2 are not known.

The molecular studies published on QR2 are rather scarce. Historical and key papers described its catalytic activity, and then its

*Abbreviations:* BSA, bovine serum albumin; FAD, flavin adenine dinucleotide; FMN, flavin mononucleotide; BNAH, *N*-benzyl dihydonicotinamide; QR2, quinone reductase 2; ESI-MS, electrospray ionization-mass spectrometry; SEC-MALS, size exclusion chromatography-multi angle light scattering; ITC, isothermal titration calorimetry.

* Corresponding author. Tel.: +33 1 55 72 27 48; fax: +33 1 55 72 28 10.
*E-mail address:* jean.boutin@fr.netgrs.com (J.A. Boutin).

1387-3806/$ – see front matter © 2011 Elsevier B.V. All rights reserved.
doi:10.1016/j.ijms.2011.07.011

first crystallisation as well as some data on its enzymatic mechanisms [4,5,10]. Later on, stopped-flow experiments enhanced our knowledge of the mechanisms of action of the enzyme [11]. Finally, a handful of compounds (resveratrol, melatonin, catechol, 5-methoxycarbonylamino-*N*-acetyltryptamine (MCA-NAT), *N*-[2-(7-methylaminosulfonyl-1-naphthyl)ethyl]acetamide (S26695), *N*-[2-(2-methoxy-6H-dipyrido [2,3-*a*:3,2-*e*]pyrrolizin-11-yl)ethyl]-2-furamide (S29434) were co-crystallized with QR2 [12–15].

Our own studies of QR2 included the discovery of potent inhibitors such as S 26695 and S 29434 and others [16–18]. Some of these compounds have shown activities on the inhibition of memory loss [19], opening up a whole field of new investigations.

The basic knowledge on the relationship between QR2 and its potent inhibitors remains poor and sometimes complex to understand (see [17,18,20]). Therefore, we started a series of experiments using various biophysical approaches, including native mass spectrometry analyses and fluorescence spectroscopy, to complete our understanding of the molecular feature of human recombinant QR2.

In the present paper, we applied native ESI-MS and fluorescence spectroscopy to the study of the binding of FAD and inhibitors onto QR2. This is the first time native mass spectrometry was used to characterize the relationship between the enzyme and its inhibitors and its natural cofactors (whether zinc atom or FAD). These experiments demonstrate the strong potential of native mass spectrometry for deciphering the strength and the stoichiometry of enzyme-cosubstrate/inhibitor complexes.

## 2. Materials and methods

### 2.1. Reagents and chemicals

Acetonitrile, water, ammonium acetate and formic acid were mass-spectrometry grade, they were obtained from Sigma (St. Louis, MO, USA) as well as FAD, melatonin (*N*-acetyl-5-methoxytryptamine), menadione, resveratrol, horse heart myoglobin, and monomeric bovine serum albumin. *N*-benzyl dihydonicotinamide (BNAH) was from BioMol (Enzo Life Sciences Inc, Farmingdale, NY, USA). S26695 (*N*-[2-(7-methylaminosulfonyl-1-naphthyl)ethyl]acetamide) was synthesized in-house as described [17]. Melatonin, menadione, resveratrol and S26695 were solubilized to 10 mM in anhydrous EtOH. FAD was dissolved in water and quantified spectrophotometrically using an extinction coefficient of 11,300 $M^{-1}$ $cm^{-1}$ at 450 nm.

### 2.2. Cloning, expression and purification of human QR2

This work was outsourced to Protenia SA (Ifrane, Morocco). In brief, the human QR2 cDNA was obtained by PCR amplification from the pcDNA3.1(+)/hQR2 plasmid [21] and subcloned in the pFastBac1 vector (Invitrogen, Carlsbad, CA, USA). DH10Bac cells were transformed by pFastBac/hQR2 to generate the Bac-hQR2 bacmid, following the recommendations of the manufacturer. Sf9 cells in SFM medium were transfected by the Bac-hQR2 bacmid. After five days, the medium was centrifuged and the recombinant baculovirus contained in the supernatant were titrated and amplified to obtain a large stock of virus ($5 \times 10^6$ pfu/mL). For the QR2 production, Sf9 cells grown in 1.5 L of PFM medium at 28 °C to $2 \times 10^6$ cells/mL were infected by 45 mL of recombinant baculovirus. Cells were harvested after 3 days. The pellet was suspended and lyzed in buffer A (25 mM Tris/HCl, 10 mM NaCl, 1 mM DTT) supplemented with 1 mM PMSF, 1 μm pepstatin A, 10 μM EDTA. After centrifugation (18,000 rpm, 15 min, 4 °C), the supernatant was applied to XK50/20 Fast Flow DEAE column equilibrated with buffer A and washed with a linear gradient of buffer B (Buffer A with 1 M NaCl). Fractions containing the enzyme (detected by SDS–PAGE) were pooled and concentrated. The concentrated enzyme solution was then diluted in buffer A and applied to an XK26-40 Source 15Q column equilibrated with buffer A. The enzyme was eluted with a linear gradient of buffer B. Elution was monitored by measuring the absorbance at 280 and 392 nm. Two peaks containing QR2 were resolved and pooled independently. Both pools were concentrated to 5–6 mg/mL and buffer-exchanged on Centricon devices (10 kDa cut-off) with buffer C (50 mM Tris/HCl, pH 8.0, 150 mM NaCl, 10% glycerol). Concentrated QR2 solutions were aliquoted, flash-frozen and stored at −80 °C. QR2 was quantified by measuring absorbance at 280 nm using an extinction coefficient of 44,620 $M^{-1}$ $cm^{-1}$, giving monomer concentration.

### 2.3. Size exclusion chromatography-multi angle light scattering

An AKTA Explorer (GE Healthcare, Buckinghamshire, England) fitted with a Superdex 200 5/150 column was connected to a DAWN EOS laser light scattering instrument (Wyatt Technology Corp., Santa Barbara, CA, USA) and an Optilab rEX differential refractometer (Wyatt Technology Corp., Santa Barbara, CA, USA). The column and following detectors were equilibrated overnight with 50 mM Tris–HCl, pH 8.0, 200 mM NaCl at 0.2 mL/min. The instrument was calibrated with monomeric BSA. Protein samples were centrifuged 15 min at 13,000 × *g* and 4 °C before injection on the column. 20 μL of 1 mg/mL QR2 were injected for analysis. Data were acquired and processed with the Astra software (Wyatt Technology Corp., Santa Barbara, CA, USA), using a dn/dc value of 0.185 for BSA and QR2.

### 2.4. QR2 activity assay

The QR2 enzymatic activity was measured at 25 °C using 100 μM menadione and serial dilutions of QR2, diluted in 50 mM Tris/HCl, pH 8.5, 1 mM *n*-octyl-B-D-glucopyranoside. Reactions were started by addition of 100 μM BNAH and followed by measuring the decrease of BNAH fluorescence at 440 nm with excitation at 340 nm, using a FluoStar Omega 96-well plate reader (BMG, Offenburg, Germany). Specific activity is expressed as nmole/min/mg of protein.

### 2.5. Nano-electrospray ionization mass spectrometry

Nano-ESI mass spectra were acquired on a time-of-flight mass spectrometer (LCT Premier XE, Waters, Milford, MA, USA) upgraded with the Non-Covalent Enhancement kit and fitted with an automated chip-based NanoESI system (Nanomate 200, Advion Biosciences, Ithaca, NY, USA). Standard nanospray parameters were used throughout the study: chip voltage was set at 1500 V and gas pressure was set at 0.3 psi. Purity and homogeneity of the QR2 samples were checked by mass spectrometry in denaturing conditions. Proteins were desalted by reversed-phase chromatography in acetonitrile/water/formic acid (50:50:1) with ZipTip C4 pipette tips following manufacturer instructions (Millipore, Billerica, MA, USA). Mass spectra were recorded in the positive ion V mode on the mass range *m/z* 500–2000, after calibration with 2 μM horse heart myoglobin dissolved in acetonitrile/water/formic acid (50:50:1, v/v). Before native ESI-MS measurements, QR2 samples were desalted in 200 mM ammonium acetate (pH 7.5) by three successive buffer-exchange steps with Zeba Spin Desalting Columns (7 kDa cut-off, Pierce, Rockford, IL, USA). ESI-MS measurements of QR2 samples in native conditions were performed in 200 mM ammonium acetate (pH 7.5). QR2 was diluted to 10 μM (monomer concentration). When compounds solubilized in EtOH were added, final EtOH concentration never exceeded 2.5%. The mass spectrometer was carefully tuned with gentle desolvation parameters to maintain

non-covalent complexes intact during the ionization/desorption process. The cone, ion guide 1 and aperture 1 voltages were optimized to 50 V, 50 V and 10 V, respectively. The pressure in the source region was increased to 2.4 mbar. Ions were detected with a multichannel plate (MCP) detector set at 2200 V. Native mass spectra were recorded in the positive V mode on the mass range $m/z$ 500–5000 after calibration with 2 μM horse heart myoglobin dissolved in acetonitrile/water/formic acid (50:50:1, v/v). Data were acquired and processed using MassLynx v4.1 (Millipore, Billerica, MA, USA). Spectra acquired for 1–2 min were combined and smoothed before centering.

### 2.6. Quantification of QR2-bound FAD by UV–Vis spectroscopy

FAD content of Pool2 QR2 was estimated by UV–Vis spectroscopy after SDS denaturation of the enzyme, as described by Aliverti et al. [22]. Briefly, the UV–Vis spectrum of 16 μM QR2 (monomer concentration) in 50 mM Tris/HCl, 250 mM NaCl, pH 8.0 was recorded on a UVmc2 spectrophotometer (SAFAS, Monaco) in a 1 mL quartz cuvette. After addition of 0.2% SDS, spectra were recorded until modification of the FAD spectra stopped (3 h incubation). Concentration of free FAD was then estimated from the absorbance at 450 nm, using an extinction coefficient of 11,300 $M^{-1}$ $cm^{-1}$.

### 2.7. Equilibrium binding of FAD to deflavo-QR2

Fluorescence measurements were performed at 25 °C on a Xenius FLX spectrofluorometer (SAFAS, Monaco), using 1 mL quartz cuvettes. FAD binding to deflavo-QR2 induces a strong quenching of the intrinsic Trp fluorescence emission. FAD binding to deflavo-QR2 was monitored by measuring the QR2 fluorescence emission spectra after incubation of 1 μM deflavo-QR2 (monomer concentration) with increasing FAD concentrations (0–2.5 μM) in 50 mM Tris, 250 mM NaCl, pH 8.0, under light stirring. Excitation was set at 280 nm to observe emission from 300 to 450 nm. Maximum emission values were corrected for dilution, plotted as a function of total FAD concentration and fitted to the one-binding site quadratic equation (1), with $F_{obs}$ representing observed fluorescence, $F_{comp}$, the fraction of the FAD/QR2 complex, $f_c$, fluorescence level of the FAD/QR2 complex, $f_{QR2}$, fluorescence level of apo-QR2, $K_D$, dissociation constant of the FAD/QR2 complex, [FAD], total concentration of FAD, [QR2], total concentration of QR2. Nonlinear least-square regression analysis was performed with Prism (v5.03, GraphPad, LaJolla, CA, USA).

$$F_{obs} = F_{comp} f_c + (1 - F_{comp}) f_{QR2}$$
$$F_{comp} = \frac{K_D + [QR2] + [FAD] - \sqrt{(K_D[QR2] + [FAD])^2 - 4[QR2][FAD]}}{2[QR2]} \quad (1)$$

### 2.8. Reconstitution of the flavo-QR2 from Pool1 and Pool2 QR2

As-isolated Pool1 and Pool2 QR2 samples were incubated with a slight molar excess of FAD for 2 h at room temperature. Unbound FAD was removed by three successive desalting steps with Zeba Spin Desalting Columns (Pierce, Rockford, IL, USA).

## 3. Results

### 3.1. Purification and oligomeric state of QR2

#### 3.1.1. Purification

Soluble untagged wild-type QR2 was successfully expressed in high yield in Sf9 cells. Approximately 40 mg of 95% pure QR2 was obtained per liter of culture. The final step of the purification procedure allowed for the separation of two resolved peaks of QR2. Pool1 eluted first from the Source 15Q column and appeared transparent while Pool2 eluted later and appeared pale yellow, as confirmed from the 280 nm and 392 nm chromatogram (Fig. 1). This observation strongly suggested that Pool1 corresponds to FAD-free QR2 (referred to as deflavo-QR2), while Pool2 corresponds to FAD-containing QR2.

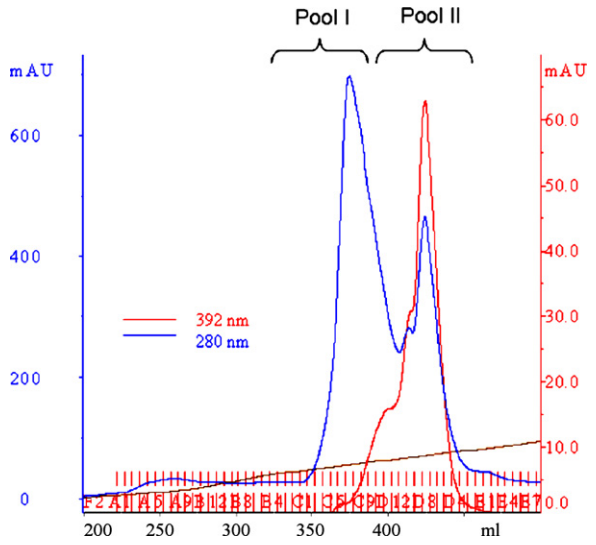


**Fig. 1.** Chromatogram of the separation of Pool1 and Pool2 QR2 by ion-exchange chromatography. Elution of QR2 from the Source 15Q column was monitored by the protein absorbance at 280 nm (blue curve) and the FAD absorbance at 392 nm (red curve).

#### 3.1.2. Oligomeric state

Oligomeric state and homogeneity of Pool1 and Pool2 was assessed by SEC-MALS analysis. Pool1 and Pool2 QR2 eluted from the column as a major symmetrical peak with a fairly homogeneous molecular weight distribution. Two minor high molecular weight peaks were observed for Pool2 (Supplementary Fig. 1). Calculated molecular weights were 57 kDa for both Pool1 and Pool2. The theoretical molecular weight of monomeric QR2 being 25.9 kDa, the SEC-MALS results showed that both QR2 pools are dimeric.

### 3.2. Biochemical and enzymatic characterization of FAD-binding to QR2

#### 3.2.1. QR2-bound FAD quantification

Visible absorption spectroscopy was used to estimate the presence and concentration of bound FAD in Pool1 and Pool2. As expected, the yellow Pool2 featured the typical visible spectrum of an oxidized flavin-containing protein, with maxima at 390 and 454 nm. Those spectral features were absent from Pool1, supporting the absence of FAD in this Pool1 QR2 (data not shown). Quantification of FAD released after SDS-denaturation of Pool2 QR2 (3 h incubation) revealed a sub-stoichiometric FAD content estimated around 0.6 FAD/QR2 monomer. Release of FAD from denatured QR2 was confirmed by the spectral shift of the 454 nm band down to 450 nm and of the 390 nm band down to 378 nm (Fig. 2), identical to the free FAD absorption maxima recorded in the same buffer (data not shown).

#### 3.2.2. Evaluation of FAD binding to deflavo-QR2

The addition of FAD to deflavo-QR2 (Pool1) led to a strong quenching of the fluorescence of the protein tryptophans (Fig. 3). This spectroscopic feature was used to assess the dissociation constant of FAD. Sequential titration of QR2 with FAD revealed the tight

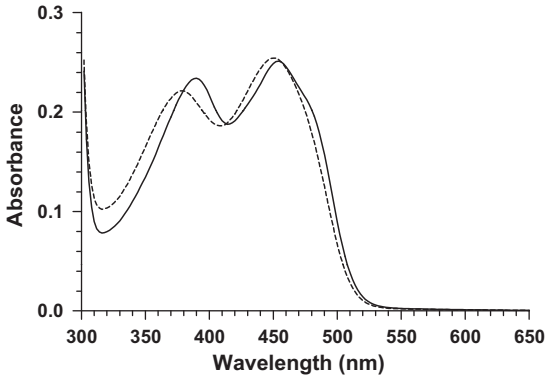


**Fig. 2.** Electronic absorption spectrum of Pool2 QR2 as-isolated (solid line), and after SDS-denaturation (dashed line). QR2 monomer concentration was 16 μM, in 50 mM Tris, 250 mM NaCl, pH 8.0. Final SDS concentration was 0.01%.

binding of the cofactor to the enzyme, governed by an apparent $K_D$ of 48 ± 10 nM, with a stoichiometry of one FAD molecule per QR2 monomer.

### 3.2.3. Activity assays

The enzymatic activity of Pool1 and Pool2 QR2 was assayed before and after reconstitution with FAD. As-isolated Pool1 displayed a specific activity of 5300 nmol/min/mg, corresponding to a $k_{cat}$ of 2 $s^{-1}$, whereas as-isolated Pool2 featured 137,700 nmol/min/mg, corresponding to a $k_{cat}$ of 60 $s^{-1}$. After reconstitution with FAD, Pool1 and Pool2 showed increased activity with similar specific activity of 369,600 and 380,000 nmol/min/mg, respectively, corresponding to $k_{cat}$ values of 160 and 165 $s^{-1}$.

### 3.3. Native ESI-MS study of as-isolated and reconstituted QR2 samples

Prior to native MS experiments, the exact mass of intact Pool1 and Pool2 QR2 was checked by denaturing ESI-MS (Fig. 4). Under the condition used, a broad distribution of high charge states was observed, consistent with ions of unfolded QR2. Moreover, a second envelope of low charge states centered around the $z = 11$ ion suggests the presence of a population of more compact, native-like QR2 monomers. The following molecular weights were measured: 25864.1 ± 0.6 Da for Pool1 and 25865.1 ± 0.3 Da for Pool2. These two virtually identical molecular weights are 89 Da smaller than the 25,952 Da calculated from the sequence of the full-length QR2, and 43 Da higher than the 25821.3 Da expected for the N-terminal Met-truncated QR2. This 43 Da covalent adduct is compatible with the N-terminal acetylation of the N-terminal Met-truncated QR2.

As-isolated Pool1 and Pool2 QR2 were then analyzed in their native form by native ESI-MS (Fig. 5). For Pool1 QR2, a single species was observed, with a charge state distribution in the 3400–4200 $m/z$ range. Calculated molecular weight was 51,857 Da, in very good agreement with the 51,856.8 Da expected for a QR2 dimer containing 2 zinc atoms, each chelated by a deprotonated Cys (25,864 × 2 + 65.4 × 2 − 2 Da). No monomers or dimers without Zn were observed (Fig. 5A).

For Pool2 QR2, a similar charge state distribution was observed. Moreover, a closer inspection of the spectra revealed that each charge state was composed of five different species. Barely detectable QR2 dimer with 2 Zn was found at 51,857 Da. The most intense ion was detected at 53,429 Da, representing a 1572 Da adduct to the QR2-Zn dimer. This species corresponds nicely to the QR2-Zn dimer with two FAD bound (53,427 Da: 51,857 + (2 × 785) Da). The second most intense ion, observed at 52,641 Da, corresponds to the QR2-Zn dimer with only one FAD bound (52,642 Da: 51,857 + 785 Da). Between those two FAD-bound QR2 was found an unexpected species at 53,099 Da, compatible with a QR2-Zn dimer containing one FAD and one FMN (53,098 Da: 51,857 + 785 + 456 Da). Finally, a lowly populated ion was detected at 52,315 Da, corresponding to a QR2-Zn dimer containing one FMN (52,313 Da: 51,857 + 456 Da) (Fig. 5B).

Native ESI-MS analysis of Pool1 and Pool2 after reconstitution with FAD gave very similar spectra featuring a single species of 53,429 Da, corresponding to the QR2-Zn dimer with two FAD bound. FMN adducts were not observed with reconstituted QR2 from Pool2 (Fig. 5, cases A4 and B4).

### 3.4. Native ESI-MS study of substrates and inhibitor binding to QR2

Native ESI-MS was further used to study the binding of known co-substrates and inhibitors of QR2. Menadione and BNAH are co-substrates for QR2. BNAH reduces the oxidized FAD to generate two-electrons reduced FAD able to reduce menadione to menadiol. Melatonin, resveratrol and S26695 are potent inhibitors of QR2. All these five aromatic molecules are described to bind at the active site. Menadione, melatonin and resveratrol have been co-crystallized with the enzyme, revealing a binding mode relying primarily on stacking with the isoaloxazine ring of bound FAD [10,13,15].

Inhibitors binding to deflavo-QR2 (Pool1), as-isolated Pool2, FAD-reconstituted Pool1 and FAD-reconstituted Pool2 were assessed with 20 μM inhibitors (Fig. 6). Similar results were obtained for melatonin (232 Da), resveratrol (228 Da) and S26695 (306 Da). On one hand, weak binding (<20%) of one inhibitor per dimer was observed with deflavo-QR2 (Fig. 6A). Weak complexes were observed at 52,090 Da with melatonin, 52,087 Da with

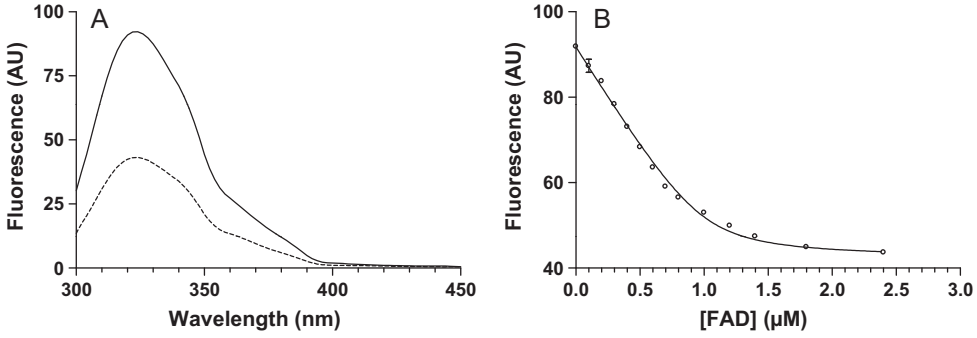


**Fig. 3.** Equilibrium binding of FAD to deflavo-QR2 (Pool1), monitored by QR2 intrinsic fluorescence emission, in 50 mM Tris, 250 mM NaCl, pH 8.0. (A) Fluorescence emission spectra of 1 μM QR2 (monomer concentration), before (solid line) and after incubation with 2.5 μM FAD (dashed line), recorded from 300 to 450 nm with excitation fixed at 280 nm. (B) Binding profile of FAD to deflavo-QR2. The line is a fit to the one binding-site Eq. (1), with $K_D$ = 48 ± 10 nM.

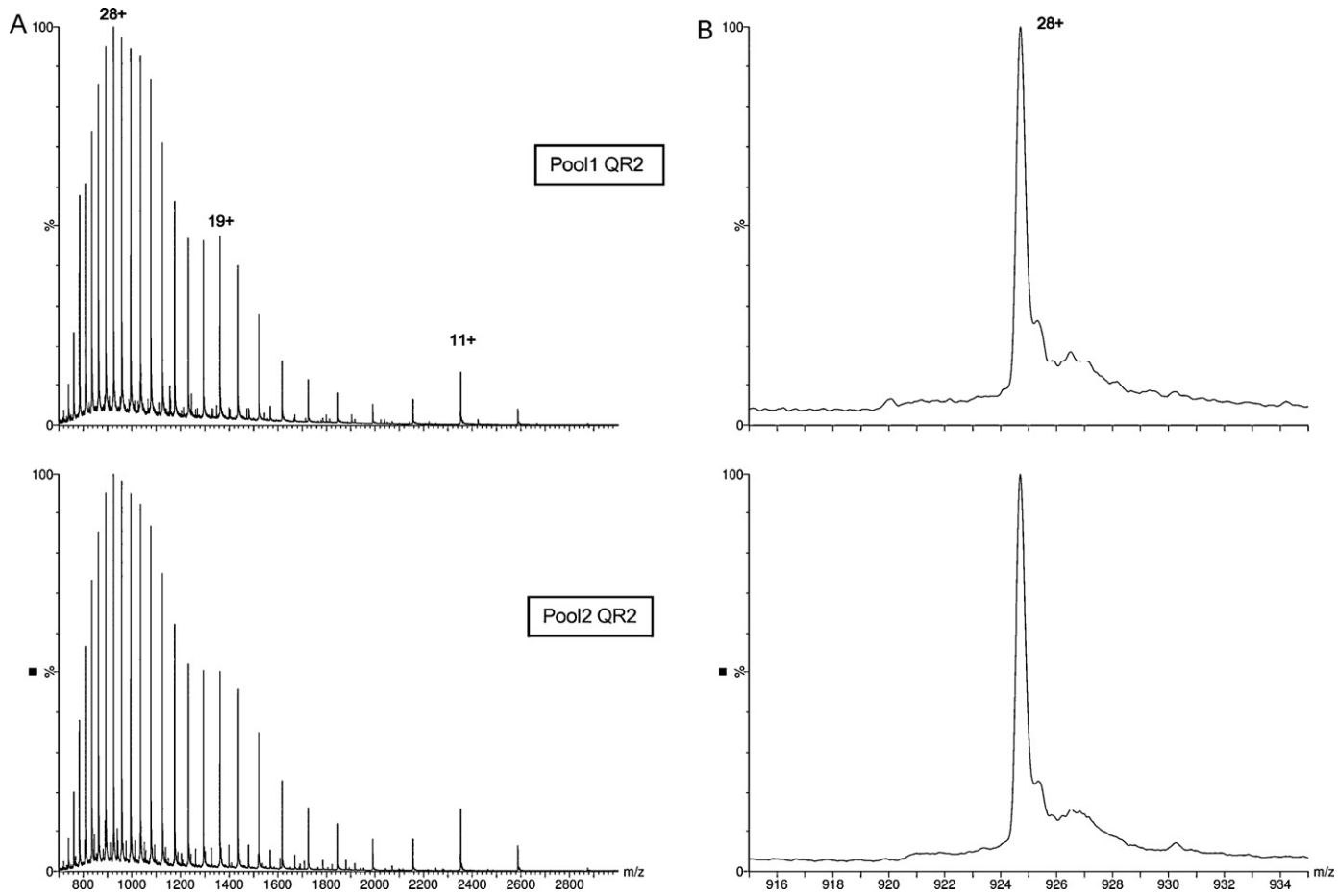


**Fig. 4.** Nano-ESI mass spectra of as-isolated Pool1 and Pool2 QR2 under denaturing conditions (50% acetonitrile/50% $H_2O$/1% formic acid). (A) Full-scale spectra of as-isolated Pool1 QR2 (upper frame) and as-isolated Pool2 QR2 (lower frame). (B) Enlargement on the $z = 28$ peak of as-isolated Pool1 QR2 (upper frame) and as-isolated Pool2 QR2 (lower frame).

resveratrol and 52,164 Da with S26695. On the other hand, almost complete binding (>90%) of two inhibitors per dimer was observed with both FAD-reconstituted Pool1 and Pool2 (Fig. 6C and D). Complexes were observed at 53,894 Da with melatonin, 53,886 Da with resveratrol and 54,041 Da with S26695. Finally, almost complete binding of inhibitors was observed only to FAD or FMN-containing populations of as-isolated Pool2 (Fig. 6B). Namely, one inhibitor molecule per QR2-Zn dimer containing one FAD or one FMN (52,875 Da and 52,548 Da with melatonin, 52,869 Da and 52,544 Da with resveratrol and 52,950 Da and 52,618 Da with S26695) and two inhibitor molecules per QR2-Zn dimer containing two FAD or one FAD and one FMN were observed (53,895 Da and 53,563 Da with melatonin, 53,883 Da and 53,555 Da with resveratrol and 54,042 Da and 53,716 Da with S26695). For melatonin, a weak QR2-Zn dimer containing two FAD with a single bound melatonin was observed at 53,661 Da. For resveratrol, a weak QR2-Zn dimer containing two FAD with three bound resveratrol was observed at 54,114 Da.

Binding of the co-substrate and substrate, BNAH and menadione, was first studied at 50 μM. Addition of BNAH to deflavo-QR2 (Pool1) lead to the appearance of a minor species at 52,069 Da (<25%), compatible with the QR2-Zn dimer with only 1 BNAH bound. Addition of BNAH to the FAD-reconstituted Pool1 and Pool2 QR2 gave similar results with the appearance of two major species of 53,643 and 53,857 Da, corresponding to the holo-QR2-Zn-FAD dimer bound with one and two BNAH, respectively. A third minor species of 54,073 Da was also detected, compatible with the holo-QR2-Zn-FAD dimer bound with three BNAH molecules. The addition of BNAH to the as-isolated Pool2 QR2 leads to the appearance of 5 species at 52,644 Da, 52,858 Da, 53,644 Da, 53,859 Da and 54,073 Da, corresponding respectively to QR2-Zn dimer bound with one FMN and one BNAH, QR2-Zn dimer bound with one FAD and one BNAH, holo-QR2-Zn-FAD dimer bound with one BNAH, holo-QR2-Zn-FAD dimer bound with two BNAH molecules and holo-QR2-Zn-FAD dimer bound with three BNAH molecules. Increasing the concentration of BNAH up to 200 μM slightly increased the proportion of all BNAH-bound populations (Fig. 7). The same experiments realized with menadione failed to identify any non-covalent complexes.

## 4. Discussion

Quinone reductase 2 is a mysterious enzyme because it presents some unexpected features that remain remarkable [1,23,24]. The enzyme has been first identified in the early 1960, and then remained ignored for 30 years [4]. It was discovered again, first by Jaiswal [25] while looking for isoforms of quinone reductase 1 and then by Talalay's group [5]. The enzyme was then cloned and enzymatically studied. Its main features were reported in four historical papers [5,10–12]. We encountered QR2 in the process of finding the third melatonin binding site [21], and kept studying this enzyme for the last 10 years, including the design of several series of potent inhibitors [16,17,26–28]. Very recently, we demonstrated that powerful QR2 inhibitors such as S26695 were potent memory sustainers [19], via a mechanism suspected to be linked

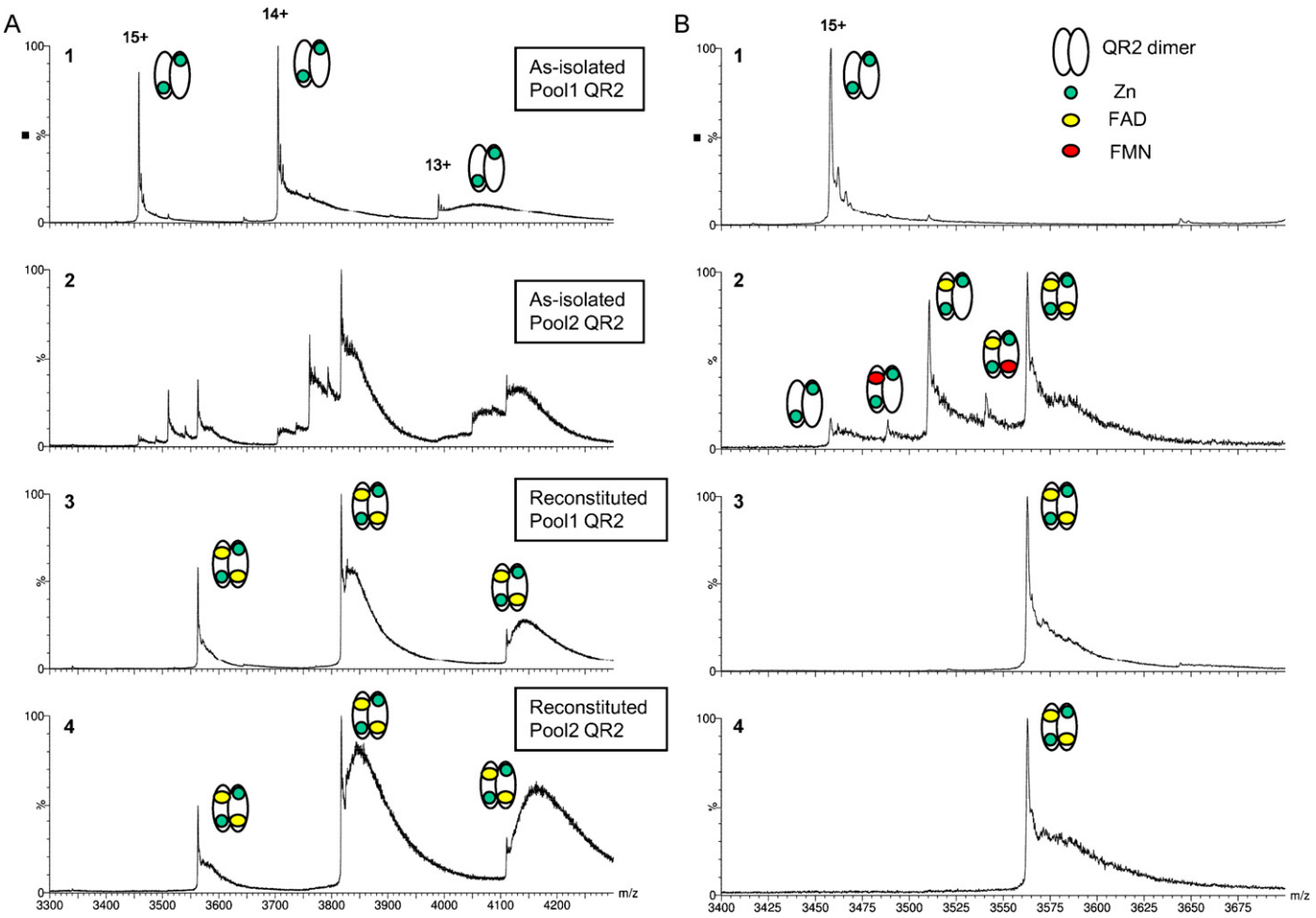


**Fig. 5.** Nano-ESI mass spectra of as-isolated and FAD-reconstituted Pool1 and Pool2 QR2 in native conditions (200 mM ammonium acetate, pH 7.5). (A) Charge states distribution of (1) as-isolated Pool1, (2) as-isolated Pool2, (3) FAD-reconstituted Pool1 and (4) FAD-reconstituted Pool2. (B) Enlargement of the $z = 15$ charge state.

to the de-regulated over-production of reactive oxygen species. It was obvious to us that more studies were necessary to better understand some of the reported features of the enzyme, particularly discrepancies due to various methods of expression and/or purification and/or assay conditions of the recombinant human enzyme. One should keep in mind that QR2 is inactive unless its co-substrates are present in the right oxidized form. The quantity and/or the conditions under which those co-substrates are produced in cells are still unknown, although some progress has been made recently [29].

The present work aimed at describing more precisely, and by using modern biophysical techniques, the behavior of the enzyme, as well as its binding of some molecules.

### 4.1. FAD binding to QR2

After production of QR2 in Sf9 cells and purification in absence of FAD, 2 populations of QR2 were isolated, namely Pool1 and Pool2. Denaturing ESI-MS unambiguously showed that Pool1 and Pool2 are identical QR2 enzymes. Moreover, MS data revealed an 89 Da difference with the expected molecular mass. This result strongly suggests that QR2 expressed in Sf9 cells has lost its *N*-terminal methionine before being *N*-acetylated on a single site. Additionally, the presence of a low-abundance population of native-like monomeric QR2 ions shows that the denaturing conditions used were not strong enough to fully denature the QR2 dimers. This observation also suggests that the QR2 momomers might represent an intermediate state in the denaturing pathway of dimeric QR2. QR2 has been described previously as a homodimer. SEC-MALS analysis of both Pool1 and Pool2 confirmed this statement, as only homogeneous dimeric form of QR2 was observed. Electronic absorption spectroscopy suggested that Pool1 QR2 is a flavin-free QR2, while Pool2 QR2 contains flavin cofactors, but in sub-stoichiometric quantities. Fluorescence spectroscopy revealed the stoichiometric binding of one FAD per Pool1 QR2 monomer, with a strong affinity ($K_D = 50$ nM), as could be expected from an FAD-dependant reductase. After proper buffer-exchange in volatile buffer and careful tuning of the mass spectrometer to preserve non-covalent complexes [30–33], QR2 gave mass spectra featuring a charge-state distribution ($z = 13$, 14 and 15) of dimeric species. This clearly shows that the conditions used were "soft" enough for QR2 to retain its folded structure and oligomeric state after transfer from the liquid to the gas-phase.

Native MS analysis revealed the absence of FAD on Pool1 QR2 and the presence of bound FAD on Pool2 QR2. Average FAD stoichiometry is estimated from the MS data to be ~0.80 FAD per monomer, based on the relative intensities of the peaks. This result is in fairly good agreement with the electronic absorption spectroscopy results. Moreover, MS provided valuable additional information by directly revealing in Pool2 the presence of two populations of QR2/FAD complex: one FAD per dimer and two FAD per dimer, the latter complex being more intense. This pattern is expected for two identical and independent binding sites. Indeed, cooperativity between two binding sites can be

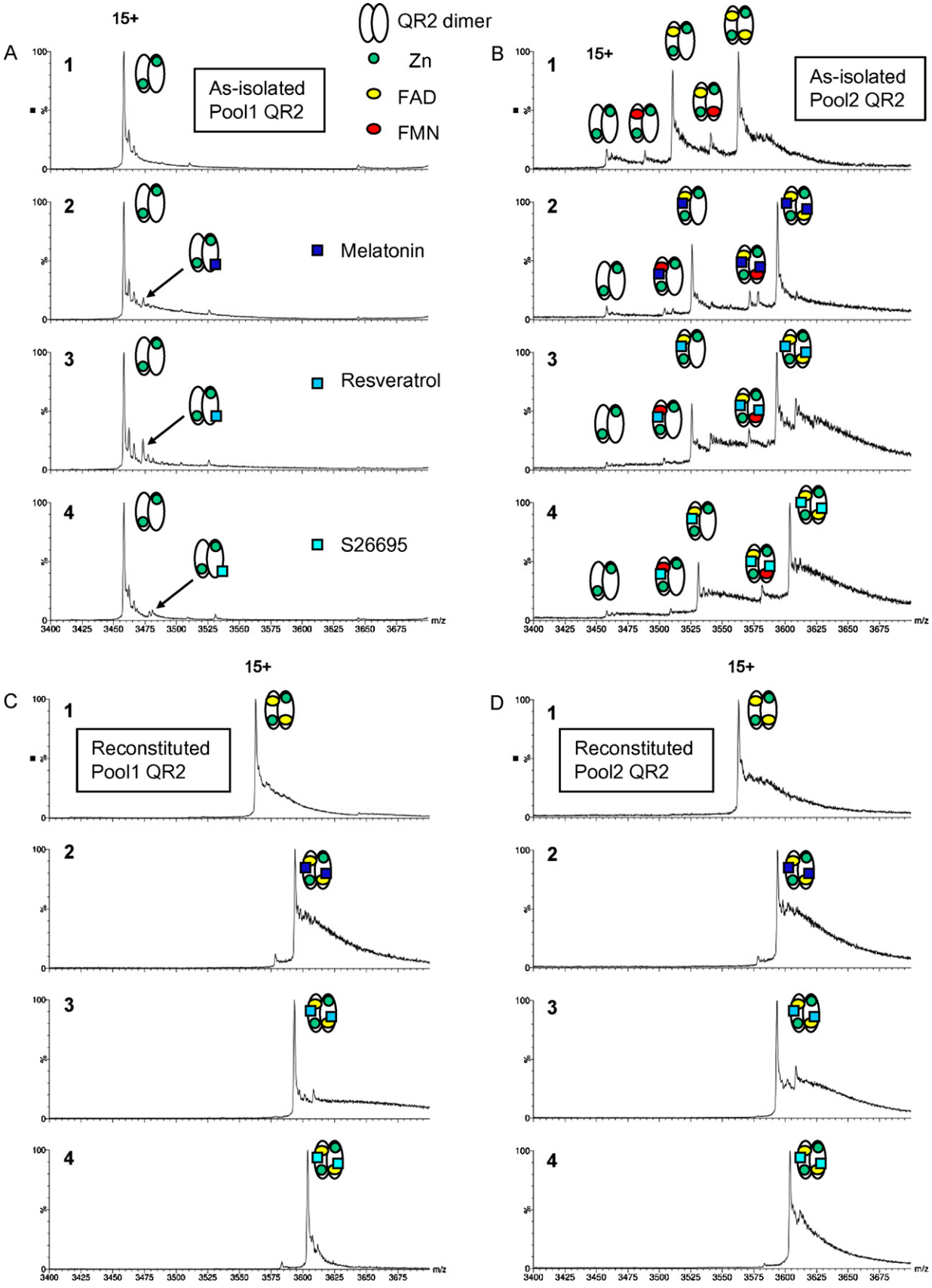


**Fig. 6.** Characterization of melatonin, resveratrol and S26695 binding to QR2 by native nano-ESI-MS: mass spectra of the $z = 15$ charge-state. (A) Inhibitors binding to deflavo-QR2 (Pool1). (1) enzyme, (2) enzyme + melatonin, (3) enzyme + resveratrol, (4) enzyme + S26695. (B) Inhibitors binding to as-isolated Pool2. (C) Inhibitors binding to FAD-reconstituted Pool1. (D) Inhibitors binding to FAD-reconstituted Pool2. QR2 concentration was 10 μM (monomer concentration), inhibitor concentration was 20 μM.

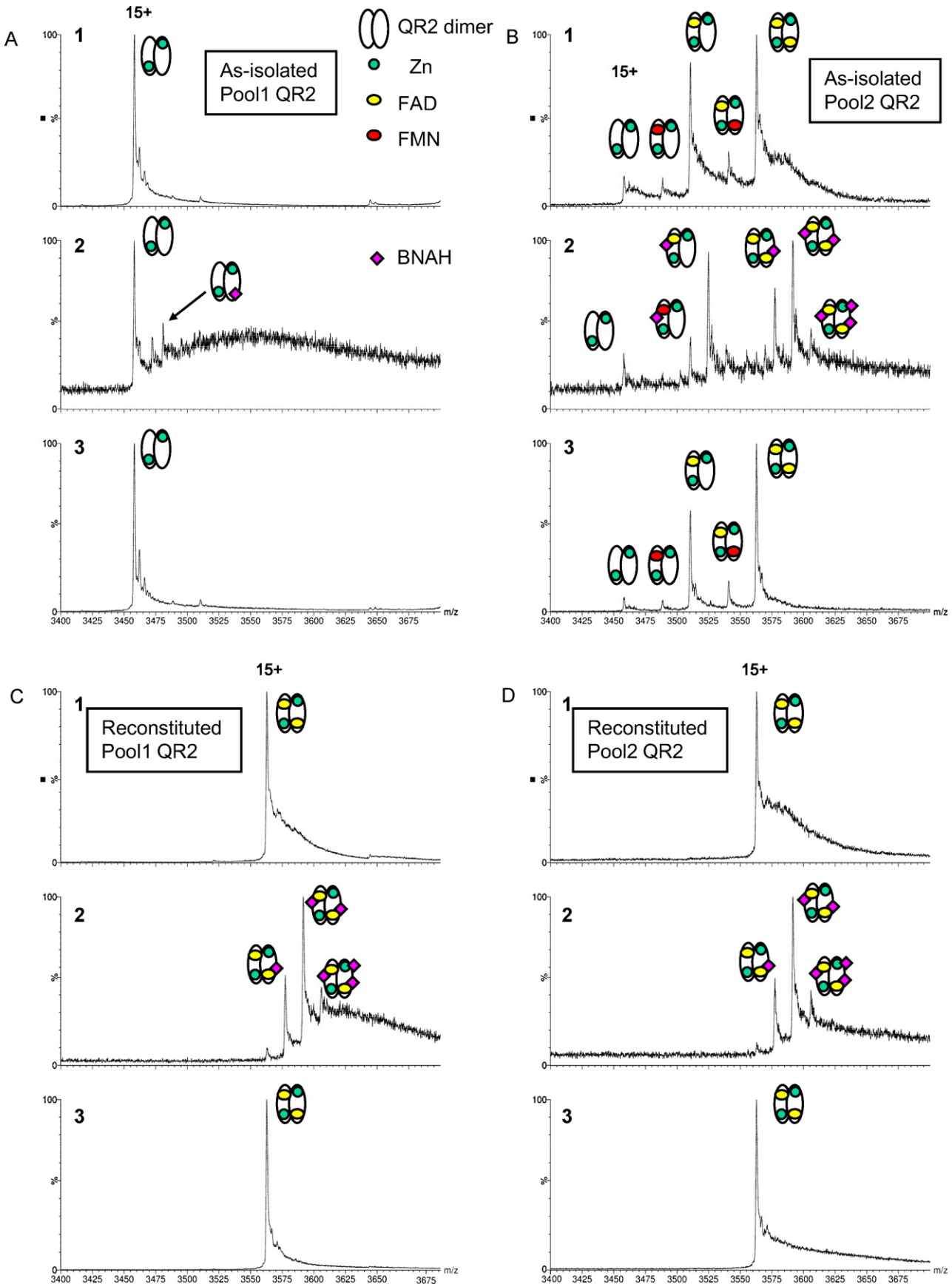


**Fig. 7.** Characterization of BNAH and menadione binding to QR2 by native nano-ESI-MS: mass spectra of the $z = 15$ charge-state. (A) Co-substrates binding to deflavo-QR2 (Pool1): (1) enzyme, (2) enzyme + BNAH, (3) enzyme + menadione. (B) Co-substrates binding to as-isolated Pool2. (C) Co-substrates binding to FAD-reconstituted Pool1. (D) Co-substrates binding to FAD-reconstituted Pool2. QR2 concentration was 10 μM (monomer concentration), co-substrates concentration was 200 μM.

reasonably well estimated from native MS data, as described by Rogniaux et al. [34] and Edwards et al. [35], using the equation $\alpha = 4 \times D0 \times D2/(D1 \times D1)$, where $\alpha$ is the ratio of $K_{FAD1}/K_{FAD2}$, with $K_{FAD1}$ and $K_{FAD2}$ being the association constants for the first and second FAD binding event respectively and D0, D1 and D2 being the fractions of unbound dimer, dimer bound to one FAD or FMN and dimer bound to two FAD or one FAD and one FMN, respectively. Applying this equation to Pool2 spectra lead to a $K_{FAD1}/K_{FAD2}$ ratio $\alpha = 0.9$, thus supporting the independent site model. This is in agreement with the fluorescence titration that was consistent with two sites of similar affinity.

It is clear from both MS and electronic absorption spectroscopy that Pool2 is not fully loaded with FAD. This is likely because of FAD shortage in the Sf9 cell during the course of the strong QR2 expression. MS data also showed the presence of low amounts of FMN bound to QR2. Bound FMN was displaced by FAD during reconstitution, suggesting a weaker affinity of FMN for QR2 compared to FAD.

As an additional remark, the separation of deflavo- and FAD-containing-QR2 by anion exchange suggested a modification of the surface charges upon FAD binding. The existence of a conformational change induced by the FAD binding is reinforced by preliminary circular dichroism experiments revealing a difference in secondary structure content between Pool1 and Pool2 (M. Antoine, G. Ferry, unpublished results). Further investigations using native MS, CD, fluorescence spectroscopy and X-ray crystallography will be required to confirm this hypothesis.

Finally, our data show that FAD is not essential for QR2 folding. Indeed, deflavo-QR2 is easily purified, has been shown to be dimeric by SEC-MALS, and gives native mass spectra revealing a compact, folded structure in the gas-phase.

### 4.2. Inhibitors binding to QR2

A set of three well-characterized QR2 inhibitors was selected to assess the potential of native ESI-MS for detecting non-covalent binding of compounds to QR2. Melatonin, resveratrol and S26695 have been co-crystallized with QR2 [13,15] and revealed the details of their interaction with the enzyme at atomic resolution. All three inhibitors were found to bind in the FAD-loaded active site, by stacking against the flavin ring and by engaging direct H-bonds with QR2 or via a relay through water molecules. When probed by native ESI-MS, melatonin, resveratrol and S 26695 were found to bind strongly and almost exclusively to flavin-containing QR2 dimers. QR2 dimers containing one flavin were able to bind one inhibitor while QR2 dimers containing two flavins bound two inhibitors. This is consistent with the reported binding mode of those compounds. Moreover, the fact that complete binding of resveratrol and melatonin was observed with 10 μM enzyme and 20 μM compound indicate that $K_D$ values for those two compounds are lower than 5 μM, in good agreement with previously reported ITC results [15].

### 4.3. Co-substrates binding to QR2

Menadione has been co-crystallized with QR2 [10]. It is clear from this structure that binding of menadione mainly involve a π–π stacking interaction between the A ring of the isoalloxazine. No strong ionic interactions nor H-bond between menadione and QR2 are observed. When probed by native ESI-MS, no binding of menadione could be measured, even with a concentration of 200 μM, which was used for the co-crystallization. This suggest that binding of menadione could mainly be driven by hydrophobic interaction that are lost in the gas-phase, in line with the crystallographic data. There is currently no structure of the BNAH-QR2 complex. However, it is very likely that the nicotinamide ring of the co-substrate would adopt a binding mode similar to that of menadione and inhibitors, stacked against the flavin ring. Consistent with this hypothesis, BNAH was found by native ESI-MS to bind predominantly to flavin-containing QR2 dimer, with the same stoichiometry as the bound flavin. Additionally, our MS data show that one BNAH is able to weakly bind to the deflavo-QR2 dimer and that a third BNAH can bind the FAD-dimer. While it is not possible to identify the binding site of BNAH on deflavo-QR2, or of the third BNAH on holo-QR2, based on the MS results alone, it is particularly tempting to think that BNAH could bind in the flavin pocket in its absence. Indeed, such a possibility could rationalize the low, but yet significant, menadione-reductase activity of the deflavo-QR2 measured in presence of BNAH. Following this hypothesis, the empty flavin pocket of deflavo-QR2 could stabilize a transient BNAH-menadione collision complex long enough to allow reduction of the quinone.

## 5. Conclusions

In summary, we used native ESI-MS to investigate both the FAD content of different populations of the flavoenzyme QR2 and the binding of substrates, co-substrates and inhibitors to its active-site. It was shown that native ESI-MS is able (1) to readily and quickly characterize in a single pass the structural integrity, the oligomeric state of QR2 and the stoichiometry of bound FAD, and (2) to detect non-covalent complexes between QR2 and its inhibitors. This opens the door for native MS-based screening and qualification of potential QR2 inhibitors. Native ESI-MS has now become a mature label-free technique, more and more widely accepted as a powerful tool for the identification and characterization of non-covalent complexes.

## Acknowledgements

We are grateful to Dr. A. Van Dorsselear and Dr. S. Sanglier for ESI-MS training.

## Appendix A. Supplementary data

Supplementary data associated with this article can be found, in the online version, at doi:10.1016/j.ijms.2011.07.011.

## References

[1] F. Vella, G. Ferry, P. Delagrange, J.A. Boutin, NRH:quinone reductase 2: an enzyme of surprises and mysteries, Biochem. Pharmacol. 71 (2005) 1–12.
[2] D.J. Long, A.K. Jaiswal, NRH:quinone oxidoreductase2 (NQO2), Chem. Biol. Interact. 129 (2000) 99–112.
[3] A.K. Jaiswal, P. Burnett, M. Adesnik, O.W. McBride, Nucleotide deduced amino acid sequence of a human cDNA (NQO2) corresponding to a second member of the NAD(P)H:quinone oxidoreductase gene family. Extensive polymorphism at the NQO2 gene locus on chromosome 6, Biochemistry 29 (1990) 1899–1906.
[4] S. Liao, H.G. Williams-Ashman, Enzymatic oxidation of some non-phosphorylated derivatives of dihydronicotinamide, Biochem. Biophys. Res. Commun. 4 (1961) 208–213.
[5] Q. Zhao, X.L. Yang, W.D. Holtzclaw, P. Talalay, Unexpected genetic and structural relationships of a long-forgotten flavoenzyme to NAD(P)H:quinone reductase (DT-diaphorase), Proc. Natl. Acad. Sci. U.S.A 94 (1997) 1669–1674.
[6] D.J. Long, K. Iskander, A. Gaikwad, M. Arin, D.R. Roop, R. Knox, R. Barrios, A.K. Jaiswal, Disruption of dihydronicotinamide riboside:quinone oxidoreductase 2 (NQO2) leads to myeloid hyperplasia of bone marrow and decreased sensitivity to menadione toxicity, J. Biol. Chem. 277 (2002) 46131–46139.
[7] V. Radjendirane, P. Joseph, Y.H. Lee, S. Kimura, A.J. Klein-Szanto, F.J. Gonzalez, A.K. Jaiswal, Disruption of the DT diaphorase (NQO1) gene in mice leads to increased menadione toxicity, J. Biol. Chem. 273 (1998) 7382–7389.
[8] F. Mailliet, G. Ferry, F. Vella, K. Thiam, P. Delagrange, J.A. Boutin, Organs from mice deleted for NRH:quinone oxidoreductase 2 are deprived of the melatonin binding site MT3, FEBS Lett. 578 (2004) 116–120.
[9] K. Reybier, P. Perio, G. Ferry, J. Bouajila, P. Delagrange, J.A. Boutin, F. Nepveu, Insights into the Redox Cycle of Human Quinone Reductase 2, Free Radic Res. (2011), doi:10.3109/10715762.2011.605788 [Epub ahead of print].
[10] C.E. Foster, M.A. Bianchet, P. Talalay, Q. Zhao, L.M. Amzel, Crystal structure of human quinone reductase type 2, a metalloflavoprotein, Biochemistry 38 (1999) 9881–9886.

[11] J.J Kwiek, T.A. Haystead, J. Rudolph, Kinetic mechanism of quinone oxidoreductase 2 and its inhibition by the antimalarial quinolines, Biochemistry 43 (2004) 4538–4547.
[12] M.A. Bianchet, S.B. Erdemli, L.M. Amzel, Structure, function, and mechanism of cytosolic quinone reductases, Vitam. Horm. 78 (2008) 63–84.
[13] L. Buryanovskyy, Y. Fu, M. Boyd, Y. Ma, T.C. Hsieh, J.M. Wu, Z. Zhang, Crystal structure of quinone reductase 2 in complex with resveratrol, Biochemistry 43 (2004) 11417–11426.
[14] Y. Fu, L. Buryanovskyy, Z. Zhang, Crystal structure of quinone reductase 2 in complex with cancer prodrug CB1954, Biochem. Biophys. Res. Commun. 336 (2005) 332–338.
[15] B. Calamini, B.D. Santarsiero, J.A. Boutin, A.D. Mesecar, Kinetic, thermodynamic and X-ray structural insights into the interaction of melatonin and analogues with quinone reductase 2, Biochem. J. 413 (2008) 81–91.
[16] M.F. Boussard, S. Truche, A. Rousseau-Rojas, S. Briss, S. Descamps, M. Droual, M. Wierzbicki, G. Ferry, V. Audinot, P. Delagrange, J.A. Boutin, New ligands at the melatonin binding site MT(3), Eur. J. Med. Chem. 41 (2006) 306–320.
[17] F. Mailliet, G. Ferry, F. Vella, S. Berger, F. Coge, P. Chomarat, C. Mallet, S.P. Guenin, G. Guillaumet, M.C. Viaud-Massuard, S. Yous, P. Delagrange, J.A. Boutin, Characterization of the melatoninergic MT3 binding site on the NRH:quinone oxidoreductase 2 enzyme, Biochem. Pharmacol. 71 (2005) 74–88.
[18] G. Ferry, S. Hecht, S. Berger, N. Moulharat, F. Coge, G. Guillaumet, V. Leclerc, S. Yous, P. Delagrange, J.A. Boutin, Old and new inhibitors of quinone reductase 2, Chem. Biol. Interact. 186 (2010) 103–109.
[19] C.E. Benoit, S. Bastianetto, J. Brouillette, Y. Tse, J.A. Boutin, P. Delagrange, T. Wong, P. Sarret, R. Quirion, Loss of quinone reductase 2 function selectively facilitates learning behaviors, J. Neurosci. 30 (2010) 12690–12700.
[20] J.A. Boutin, E. Marcheteau, P. Hennig, N. Moulharat, S. Berger, P. Delagrange, J.P. Bouchet, G. Ferry, MT3/QR2 melatonin binding site does not use melatonin as a substrate or a co-substrate, J. Pineal Res. 45 (2008) 524–531.
[21] O. Nosjean, M. Ferro, F. Coge, P. Beauverger, J.M. Henlin, F. Lefoulon, J.L. Fauchere, P. Delagrange, E. Canet, J.A. Boutin, Identification of the melatonin-binding site MT3 as the quinone reductase 2, J. Biol. Chem. 275 (2000) 31311–31317.
[22] A. Aliverti, B. Curti, M.A. Vanoni, Identifying, F.A.D. quantitating, FMN in simple and in iron–sulfur-containing flavoproteins, Methods Mol. Biol. 131 (1999) 9–23.
[23] R. Jockers, P. Maurice, J.A. Boutin, P. Delagrange, Melatonin receptors, heterodimerization, signal transduction and binding sites: what's new? Br. J. Pharmacol. 154 (2008) 1182–1195.
[24] J.A. Boutin, V. Audinot, G. Ferry, P. Delagrange, Molecular tools to study melatonin pathways and actions, Trends Pharmacol. Sci. 26 (2005) 412–419.
[25] A.K. Jaiswal, Human NAD(P)H:quinone oxidoreductase 2. Gene structure, activity, and tissue-specific expression, J. Biol. Chem. 269 (1994) 14502–14508.
[26] M. Ettaoussi, B. Peres, F. Klupsch, P. Delagrange, J.A. Boutin, P. Renard, D.H. Caignard, P. Chavatte, P. Berthelot, D. Lesieur, S. Yous, Design and synthesis of benzofuranic derivatives as new ligands at the melatonin-binding site MT3, Bioorg. Med. Chem. 16 (2008) 4954–4962.
[27] V. Leclerc, S. Yous, P. Delagrange, J.A. Boutin, P. Renard, D. Lesieur, Synthesis of nitroindole derivatives with high affinity and selectivity for melatoninergic binding sites MT(3), J. Med. Chem. 45 (2002) 1853–1859.
[28] V. Leclerc, M. Ettaoussi, M. Rami, A. Farce, J.A. Boutin, P. Delagrange, D.H. Caignard, P. Renard, P. Berthelot, S. Yous, Design and synthesis of naphthalenic derivatives as new ligands at the melatonin binding site MT(3), Eur. J. Med. Chem. (2011).
[29] L. Formentini, F. Moroni, A. Chiarugi, Detection and pharmacological modulation of nicotinamide mononucleotide (NMN) in vitro and in vivo, Biochem. Pharmacol. 77 (2009) 1612–1620.
[30] A. Schmidt, U. Bahr, M. Karas, Influence of pressure in the first pumping stage on analyte desolvation and fragmentation in nano-ESI MS, Anal. Chem. 73 (2001) 6040–6046.
[31] N. Tahallah, M. Pinkse, C.S. Maier, A.J. Heck, The effect of the source pressure on the abundance of ions of noncovalent protein assemblies in an electrospray ionization orthogonal time-of-flight instrument, Rapid Commun. Mass Spectrom. 15 (2001) 596–601.
[32] S. Sanglier, H. Ramstrom, J. Haiech, E. Leize, A. Van Dorsselaer, Electrospray ionization mass spectrometry analysis revealed a ~310 kDa noncovalent hexamer of HPr kinase/phosphatase from *Bacillus subtilis*, Int. J. Mass Spectrom. 219 (2002) 681–696.
[33] A. Tjernberg, S. Carno, F. Oliv, K. Benkestock, P.O. Edlund, W.J. Griffiths, D. Hallen, Determination of dissociation constants for protein–ligand complexes by electrospray ionization mass spectrometry, Anal. Chem. 76 (2004) 4325–4331.
[34] H. Rogniaux, S. Sanglier, K. Strupat, S. Azza, O. Roitel, V. Ball, D. Tritsch, G. Branlant, A. Van Dorsselaer, Mass spectrometry as a novel approach to probe cooperativity in multimeric enzymatic systems, Anal. Biochem. 291 (2001) 48–61.
[35] M.J. Edwards, M.A. Williams, A. Maxwell, A.R. McKay, Mass spectrometry reveals that the antibiotic simocyclinone D8 binds to DNA gyrase in a "bent-over" conformation: evidence for positive cooperativity in binding, Biochemistry 50 (2011) 3432–3440.